Arabian Journal of Chemistry (2022) **15**, 103648

King Saud University

Arabian Journal of Chemistry

www.ksu.edu.sa
www.sciencedirect.com

ORIGINAL ARTICLE

Electrochemical degradation of 2,4-Dinitrotoluene (DNT) from aqueous solutions using three-dimensional electrocatalytic reactor (3DER): Degradation pathway, evaluation of toxicity and optimization using RSM-CCD

Abdollah Dargahi [a,*], **Mehdi Vosoughi** [a,b,*], **S. Ahmad Mokhtari** [b], **Yaser Vaziri** [c], **Mortaza Alighadri** [b]

[a] *Social Determinants of Health Research Center, Ardabil University of Medical Sciences, Ardabil, Iran*
[b] *Department of Environmental Health Engineering, School of Public Health, Ardabil University of Medical Sciences, Ardabil, Iran*
[c] *Department of Environmental Health Engineering, School of Public Health, Hamadan University of Medical Sciences, Hamadan, Iran*

Received 4 September 2021; accepted 13 December 2021
Available online 18 December 2021

KEYWORDS

2,4-Dinitrotoluene (DNT);
Three-dimensional electrocatalytic reactor (3DER);
GAC and MCZ@Fe_3O_4 nanoparticles;
Evaluation of toxicity;
G/β-PbO_2 anode;
RSM-CCD

Abstract 2,4-Dinitrotoluene (2,4-DNT) has been found to be an important petrochemical compound, which is primarily employed for the synthesis of tolylene diisocyanate and the production of dyes, rubber, and explosives. Since this compound has high toxicity and carcinogenicity, the cautions should be considered when wastewater contaminated with DNTs and their derivatives is released into the environment. Thus, the object of the present study was the investigation of the 2,4-DNT degradation efficiency using the three-dimensional electrocatalytic reactor (3DER) with two different types of particle electrodes (granular activated carbon (GAC) and magnetized clinoptilolite zeolite (MCZ)@Fe_3O_4 nanoparticles)). Preparation of the graphite (G)/β-PbO_2 anode was done by electrochemically depositing PbO_2 layers on graphite sheets. The prepared graphite sheet and a stainless-steel 316 sheet (with the same dimensions) were employed as the anode and the cathode, respectively. Field emission scanning electron microscopy (FESEM), X-ray diffraction analysis (XRD), and energy-dispersive X-ray spectroscopy mapping (EDS-mapping) confirmed the successful preparation of G/β-PbO_2 anode. The surface morphology, chemical composition of

* Corresponding authors at: Social Determinants of Health Research Center, Ardabil University of Medical Sciences, Ardabil, Iran (A. Dargahi and M. Vosoughi).
E-mail addresses: a.dargahi29@yahoo.com (A. Dargahi), mvn_20@yahoo.com (M. Vosoughi).
Peer review under responsibility of King Saud University.

Production and hosting by Elsevier

https://doi.org/10.1016/j.arabjc.2021.103648

MCZ@Fe_3O_4 nanoparticles as a particle electrode were determined by scanning electron microscope (SEM) and XRD pattern. To determine the optimal conditions, we employed the response surface methodology-based central composite design (RSM-CCD) method. According to observed results, higher efficiency of 3DER was obtained by increasing the reaction time and current density and decreasing pH and the pollutant concentration. Studies highlighted the initial 2,4-DNT concentration of 23.5 mg/L, current density 4.8 mA/cm^2, pH of 4.1, electrolysis time of 50 min, particle electrodes dose = 6 g/250 cc as optimum values of parameters. The 2,4-DNT degradation efficiencies using GAC and MCZ@Fe_3O_4 nanoparticles as particle electrodes under mentioned optimal conditions were 98.6% and 96.5%, respectively. Moreover, the chemical oxygen demand (COD) and total organic carbon (TOC) removal efficiencies were 88.5% and 80.9% at the end of 50 min, respectively. Furthermore, results were indicative of an enhancement in average oxidation state (AOS) (from 1.27 to 2.36) and carbon oxidation state (COS) (from 1.27 to 3.68) in the 3DER process and a reduction in the COD/TOC ratio (from 1.81 to 1.09); these signposts the effectiveness of 3DER system for providing the biodegradability of 2,4-DNT. Considering the results, the 3DER could lead to suitable results for the degradation of wastewater containing DNT and resistant contaminants as pretreatment and has remarkable applicability for enhancing the biodegradability of wastewater.

1. Introduction

Due to the lack of water and the occurrence of environmental problems caused by the discharge of wastewater and effluents into the receiving water, wastewater treatment and the possibility of its reuse have been considered (Azizi et al., 2021; Geng et al., 2021). Among the various compounds of water pollutants, nitro-aromatic compounds are of special importance (Xu et al., 2019). Increased military and industrial activities using nitro-aromatic explosives have resulted in refocusing on environmental impact on soil, groundwater, and surface water associated with their application (Chen et al., 2021; Wang et al., 2017). For example, military maneuvers in the real environment are an important part of the armed forces training process, in which the continuous explosion of modern nitrogen-based munitions causes the spread of these pollutants widely in the environment (Xu et al., 2020; Zhang et al., 2020). Due to the environmental effects of military maneuvers, in some countries, efforts have been made to prevent these military actions (Hewitt et al., 2007). These efforts, along with increasing public awareness of environmental pollution issues, have led to greater attention being paid to the effects of military activities on the ecosystem (Ibrahim, 2017; Oh et al., 2010).

The 2,4-dinitrotoluene (2,4-DNT), which is considered as a by-product of manufacturing 2,4,6-trinitrotoluene (TNT), is a toxic and refractory chemical. 2,4-DNT, as an intermediate, is commercially employed in the production of dyes (Xiao et al., 2008). It is also used as a precursor to toluene diisocyanate in manufacturing polyurethane foams (Xu et al., 2020). In addition, it has application in explosives (as a waterproofing, plasticizing, and gelatinizing agent) and for smokeless powders (as a modifier) (Kuşçu and Sponza, 2011; Patapas et al., 2007). Exposure to this compound is associated with environmental impact, which is led to a major public concern. It exhibits toxicity to fish, invertebrates, algae, protozoa, and bacteria. The lowest observed effect concentration of this compound is 0.05 mg/L (Gong et al., 2003). Due to its abundance, toxicity, mutagenicity, and carcinogenicity, the Environmental Protection Agency (EPA) has listed DNT isomers including 2,4-Dinitrotoluene (2,4-DNT) as priority pollutants (EPA, 2000).

DNTs enter the environment mainly through the improper release and disposal of wastewater and industrial waste. EPA drinking water standards are set at 49.4 μg/L for 2,4-DNT, and the Code of Federal Regulations (CFR) sets industrial wastewater discharge standards for 2,4-DNT at 320 μg/L (Report, 2010). Exposure to DNTs poses serious risks to human health. Genetic experiments have highlighted that DNTs can possibly exhibit an important role in protein modification and DNA damage (Tchounwou et al., 2001). DNT isomers are highly toxic, mutagenic and carcinogenic, and damage the reproductive system. An increased incidence of tumors and urinary tract cancer has been observed in people who have had long-term exposure to DNTs (Rocheleau et al., 2010). 2,4-DNT has a long half-life in aqueous environments and this leads to their displacement through water currents (Health and Services, 1999). Degradation of nitro-aromatic compounds using conventional methods is usually difficult due to the presence of electron-inhibiting nitro groups (Achtnich et al., 1999). Although degradation of DNTs occurs faster in soil, this process takes more than 70 days, even if optimal conditions are available (Bradley et al., 1994). Therefore, wastewater treatment containing DNTs seems to be necessary to prevent its presence in environmental matrices and to prevent its environmental effects. Distillation (Zhao et al., 2010), electrochemical process (Jiang et al., 2018), biological method (Reddy et al., 2017), Advanced oxidation processes (AOPs) (Chen and Huang, 2019; Ma et al., 2017; Oh et al., 2010), and adsorption (Shukla et al., 2018; Zhang et al., 2013b) are the most utilized methods for the removal of 2,4-DNT from aqueous environments. The removal efficiencies of each of these treatment processes are different, and each has advantages and disadvantages. For example, in the adsorption process, only the contaminant phase changes and the contaminant enters from one environment to another. Aerobic biodegradation is not effective for nitroaromatic compounds, particularly those with multiple nitro group due to having the nitro group, which is strongly electron-

withdrawing (Reddy et al., 2017). Some treatment techniques, such as reverse osmosis and filtration, are largely able to remove contaminants. However, the effluent produced by these processes contains high concentrations of all unwanted compounds that are produced as a by-product and require secondary treatment (Venkatadri and Peters, 1993).

Recently, electrochemical technologies have provided noteworthy advancement in resolving water and wastewater problems which is due to the environmentally friendly, high versatility, and efficiency of these processes (Zhang et al., 2013a; Zhang et al., 2019). Despite these advantages, there are still limitations such as the short life of electrodes, low surface-to-volume ratio, and temperature increase during the process in these techniques (Mao et al., 2015). These limitations can be reduced by applying a three-dimensional electrochemical (3DE) process (Li et al., 2019; Sugashini and Begum, 2013). This process is very similar to its two-dimensional process in terms of electrode materials and treatment processes, but its difference is the presence of a third electrode. The third electrode, also known as a particle electrode, basically consists of granular material or a particle that is placed between two opposite electrodes. At a suitable voltage, these particles become polarized and a large number of charged microelectrodes are formed, one surface of each acting as an anode and the other surface acting as a cathode. Thus, due to the presence of particle electrodes, the 3DE process will perform better than its 2DE counterpart (Mao et al., 2015). Granular activated carbon (GAC) and Fe_3O_4 magnetic nanoparticles are more popular among the various materials used as particle electrodes due to their unique properties such as low cost, chemical stability, and high surface area (Dargahi et al., 2021b). In this study, the third dimension includes GAC and magnetized clinoptilolite zeolite (MCZ)@Fe_3O_4 nanoparticles and the anode is graphite (G)/β-PbO_2. These electrodes are more widely used due to advantages such as easier preparation by electrodeposition (32), low electrical resistance, availability, and good electrochemical activity. In addition, they are stable at high potentials and media with different pH. The combination of Fe_3O_4 nanoparticles with adsorbents such as MCZ to produce a magnetic carbon-based composite provides the advantages of a large specific surface area and high electrical conductivity that can promote the efficiency of Fenton-based processes by improving iron species leaching (Dargahi et al., 2021b; Tian et al., 2021; Wang et al., 2020; Yin et al., 2021).

To estimate the reaction of aquatic organisms for measurement of the impact of one or more toxins, wastewater, or environmental factors alone and together, toxicity assessment is employed. In the lower toxicity of an aqueous solution, better growth conditions for aquatic organisms are achievable. Due to characteristics reported for the use of microorganisms for bioassay such as simplicity of operation and high practical value, need for fewer laboratory facilities, and costs, the mentioned method was employed in this research. Since 2,4-DNT has been associated with risks based on the above-mentioned subjects, the aim of conducting the present study was the assessment of a three-dimensional electrocatalytic reactor (3DER) using two different types of particle electrodes (GAC and MCZ@Fe_3O_4 nanoparticles) and G/β-PbO_2 anode for 2,4-DNT degradation efficiency. Furthermore, a significant improvement in the efficiency of the oxidation process, due to the synergy of pollutant adsorption on GAC and MCZ@Fe_3O_4 nanoparticles and its electrochemical degradation in the 3DER, is expected. Moreover, determination of optimal conditions was carried out using response surface methodology based central composite design (RSM-CCD), and after that, evaluation of the kinetics of 2,4-DNT degradation, degradation pathway, and toxicity by microorganisms in the 3DER was considered. In addition, the characteristics of MCZ@Fe3O4 nanoparticles and G/β-PbO_2 anode in the present study were analyzed by X-ray diffraction analysis (XRD), scanning electron microscopy (SEM), field emission scanning electron microscopy (FESEM), EDS, and energy-dispersive X-ray spectroscopy mapping (EDS-Mapping) techniques.

2. Materials and methods

2.1. Materials

2,4-Dinitrotoluene (2,4-DNT), (the chemical formula of $C_8H_6Cl_2O$ and the purity of 99%) with a molecular weight of 182.14 g/mol, sodium hydroxide (NaOH) and Hydrochloric acid (HCl), Sodium Sulfate (Na_2SO_4, 99% purity), Lead nitrate ($Pb(NO_3)_2$, greater than99% purity), nitric acid (HNO_3, 95% purity), granular activated carbon (GAC, a diameter of 0.8–2.0 mm and specific surface area of 844.09 m^2/g), and other chemicals used were provided by Sigma Aldrich (St. Louis, MO, USA). The chemical structure of 2,4-DNT and other information about it was represented in Table S1. It should be mentioned that the analytical grade of all chemicals used in this study was employed and further purification was not applied for them. Preparing the solutions was done using double distilled water. To regulate the solution pH, 0.1 M HCl and 0.1 M NaOH were employed.

2.2. Electrode preparation

Preparing the G/β-PbO_2 anode was done through electrochemical deposition of PbO_2 layers on graphite sheets (dimensions of 8 cm × 4 cm × 0.3 cm), which is as follows: at first, we sonicated the polished graphite sheets in 40% NaOH solution for 15 min and continued the sonication process for in a 1:1 (V/V) HNO_3/H_2SO_4 mixture another 15 min. After that, the electrochemical deposition process was done in a simple cell containing 0.5 M $Pb(NO_3)_2$ and 0.1 mol/ L HNO_3 at a constant current. In the studied process, the prepared graphite sheet and the stainless-steel sheet (with the same dimensions) were employed as the anode and the cathode, respectively. Afterward, at a constant current of 7.5 mA/cm^2 for 180 min at room temperature, the PbO_2 film was deposited on the anode, and lastly, the prepared G/β-PbO_2 anode was washed several times with deionized water (Dargahi et al., 2018; Samarghandi et al., 2020).

2.3. Characterization of G/β-PbO_2 anode

Through the employment of FESEM (model: FEI-Nova NanoSEM 450) and EDS (model: Bruker XFlash6L10) analysis, the surface morphology and chemical composition of the G/β-PbO_2 anode were evaluated. Moreover, XRD (model: Ultima IV, Rigaku) was employed for identifying the phase type and crystallite structure of PbO_2 film.

2.4. Synthesis of MCZ@Fe_3O_4 nanoparticles

2.4.1. Preparation of zeolite

Clinoptilolite natural materials were obtained from mines in Kerman province. The adsorbent was first sieved with standard American Standard Test Sieve Series (ASTM) sieves (0.3–2.3 mm) and then washed with distilled water to separate impurities. The adsorbent was then dried in an oven (at 105 °C for 24 h).

2.4.2. Synthesis of Fe_3O_4 nanoparticles

Fe_3O_4 nanoparticles were synthesized by the chemical co-precipitation method. In this method, 5.4 g of $FeCl_3{\cdot}6H_2O$ and 2.78 g of $FeCl_2{\cdot}4H_2O$ (by weight per barrel) in a volume of 100 mL of water without ions were first mixed in a round bottom balloon in an atmosphere of nitrogen gas. Then, 25% ammonia solution was added dropwise to the solution on a shaker until reaching pH of the solution to 9, and finally, a black precipitate containing magnetite nanoparticles was formed. The precipitate was stirred for 30 min and heated to 80 °C, then washed three times with distilled water and finally, twice with ethanol (Yuanbi et al., 2008). After washing, a black precipitate containing magnetite particles was removed from the solution by a magnet and kept in a nitrogen gas medium until use.

2.4.3. Zeolite coating on Fe_3O_4 nanoparticles

First, 10 g of zeolite was stirred for 30 min under physical mixing with a magnetic stirrer at 200 rpm. Then, Fe_3O_4 magnetic nanoparticles were added to the mixture for loading on zeolite with a weight ratio of 10: 1, and the mixture was stirred with a magnetic stirrer at 300 rpm for 2 h. The obtained zeolite/Fe_3O_4 nanocomposite was separated by a 1.3 Tesla magnet, washed several times with distilled water, and finally dried for 12 h at 70 °C.

The surface morphology and chemical composition of the MCZ@Fe_3O_4 nanoparticles as particle electrodes were determined by SEM (model: LEO 1430VP, a joint product of England and Germany). The modified adsorbent was also structurally and chemically characterized with an XRD pattern by the X'Pert Pro diffractometer (Rigaku RINT2200, Japan).

2.5. Electrocatalytic degradation of 2,4-DNT

For conducting all electrocatalytic degradation experiments, a batch electrolytic cell (with an effective volume of 200 mL) equipped with a pair of anode and cathode was utilized. Inside the mentioned cell, the G/β-PbO_2 anode and the stainless-steel 316 (SS316) cathode (with equal dimensions) were parallelly placed at a distance of 4 cm. The third dimension of the 3DER was GAC (constant concentration of 24 gr/L), which was put in the space between the two electrodes. The two-dimensional system was created without GACs. The supporting electrolyte used in this study was Na_2SO_4 (in the different concentrations from 0.1 to 0.3 g/200 cc).

2.6. Analytical procedures

The leaching of Pb^{2+} was measured after completion of degradation of the 2,4-DNT in the studied processes using the inductively coupled plasma mass spectrometry (ICP–MS). Supplying the electrical current in this study was done using a direct current (DC) power supply (UNI-TUTP3315TFL, China) with an electric current of 0-5A and voltage of 0–30 V.

The high-performance liquid chromatography (HPLC) (Agilent Technologies Co. Ltd., USA) equipped with a C18 column (250 mm × 4.6 mm, 5 μm, Agilent) and a diode array ultraviolet detector at λ_{max} = 254 nm was employed for detecting the concentration of 2,4-DNT. The mobile phase used was a mixture of methanol/water (HPLC grade, Merck) which was used in a ratio of 70:30 at a flow rate of 1.0 mL/min with a column temperature of 25 °C. The injection volume of the 2,4-DNT was 20 μL. In addition, to measure the degradation intermediates of 2,4-DNT, the liquid chromatograph-mass spectrometer (LC-MS, Shimadzu LCMS 2010 A), which has been equipped with a C18 column (150 mm × 2.1 mm) and an electron spray ionization source, was used. a mixture of 60/40 (v/v) Acetonitrile (ACN) + 0.1% formic acid and H_2O + 0.1% formic acid was employed as mobile phase for LC-MS. Under following conditions including Mode, ESI+, Detection gain,1.8 kV, Prob Volt, 4 kV, CDL Volt, 25 V, Gas nebulizer, N_2 (grade 5), Flow gas, 1.2 L/min, CDL temperature, 270 °C, and Block temperature, 270 °C, the Mass spectra (MS) was done.

Hach pH meter (HQ430D, USA) was the device that was used to determine pH, and TOC analyzer (Elementar Analysen systeme GmbH, Germany) was employed for assessing total organic carbon (TOC). Chemical oxygen demand (COD) tests were fulfilled using COD Cell Test Method (photometric 25–1500 mg/L Spectro quant® (Merck KGaA, Darmstadt, Germany) and visible light spectrophotometry (Hach spectrophotometer DR 6000)). Other parameters, e.g., the biodegradability of 2,4-DNT, COD/TOC ratio, carbon oxidation state (COS), and the average oxidation state (AOS) have been considered in this study and were appraised under optimal conditions at room temperature.

Following equations, i.e., Eqs. (1 and 2) (Liu et al., 2020) were employed for estimating efficiency and kinetics of 2,4-DNT removal in 2D and 3D electrocatalytic oxidation systems:

$$\eta(\%) = \frac{[\mathrm{DNT}]_0 - [\mathrm{DNT}]_t}{[\mathrm{DNT}]_0} \times 100 \quad (1)$$

$$\ln\frac{[\mathrm{DNT}]_t}{[\mathrm{DNT}]_0} = -k_{obs} \times t \quad (2)$$

In above equations, η, $[\mathrm{DNT}]_0$, and $[\mathrm{DNT}]_t$ indicate the removal efficiency (%), the concentration of 2,4-DNT (mg/L) at t = 0 min, and the concentration of 2,4-DNT (mg/L) t = t min, respectively. k_{obs} is representative of pseudo-first-order kinetic coefficient (min^{-1}) and t is reaction time (min). Calculating the synergistic effect of GAC and the electrochemical degradation process was done using Eq. (3) (Pedersen et al., 2019).

$$\mathrm{Synergy}(\%) = \frac{k_{2D} - k_D}{k_{2D}} \times 100 \quad (3)$$

k_{2D}, is the kinetic coefficients of 2,4-DNT removal in 3D and k_D is the kinetic coefficients of 2,4-DNT removal in 2D electrochemical oxidation systems.

2.7. Response surface methodology (RSM) and experimental design

The optimization of parameters considered for the present study was done using response surface methodology (RSM) with the central composite design (CCD) technique. RSM is a collection of mathematical and statistical methods. It is employed to model and analyze a process in which the desired response can be affected by a number of variables. In fact, through the employment of RSM, the optimum operating conditions or a region for the factors in which certain speciation are met is determined (Seidmohammadi et al., 2021). Routinely, the linear, interactive, and quadratic effects of independent variables on the system response at five levels ($-\alpha$, -1, 0, $+1$, $+\alpha$) (Heidari et al., 2021) are evaluated by the mentioned method. The independent variables selected in the present study were the initial solution pH (A), electrolysis time (coded as B), current density (coded as C), and 2,4-DNT concentration (coded as D) (Table 1). To determine the effect of different parameters on electrocatalytic degradation of 2,4-DNT, pH in the range of 3–11, electrolysis time in the range of 15–75 min, current density in the range of 1–5 mA/cm^2, and 2,4-DNT concentration in the range of 10–90 mg/L was investigated. The statistical data analysis was performed using the Design Expert Software (version 11). By assessing achieved experimental responses for fitting a second-order polynomial model, a functional numerical relationship between the process variables and responses was established as shown in Eq. (4) (Afshin et al., 2021; Dargahi et al., 2021c).

$$Y = \beta_0 + \beta_i X_i + \beta_j X_j + \beta_{ii} X_i^2 + \beta_{jj} X_j^2 + \beta_{ij} X_i X_j + \varepsilon \quad (4)$$

In the mentioned equation, Y is indicative of response percentage of 2,4-DNT degradation, X_i, X_j indicate the k number of variables, β_i, β_{ii}, β_{ij} represent coefficients of linear, quadratic, and interaction terms respectively, and ε represents the model error. Random error (ε) articulates the measure of the difference between observed and predicted values. The experimental results were fitted to the regression model and model

Table 1 Experimental ranges and levels of the independent variables, and results of Central composite design (CCD) of experiment along with actual and predicted values of 2,4-DNT degradation.

Experimental factors and their levels							
Independent Variables	Symbol	Unit	$-\alpha$	-1	0	$+1$	$+\alpha$
pH	A	–	3	5	7	9	11
Electrolysis time	B	min	15	30	45	60	75
Current density	C	mA/cm^2	1	2	3	4	5
2,4-DNT concentration	D	mg/L	10	30	50	70	90
Results of CCD							
Run	A	B	C	D	**2,4-DNT degradation (%)**		
					Y_{exp}	Y_{pre}	ε
1	9	30	30	2	60.3	60.2	0.10
2	7	45	50	3	72.5	71.7	0.76
3	5	60	30	2	84.6	83.8	0.75
4	5	60	70	4	80.6	80.4	0.20
5	9	30	30	4	68.9	69.1	−0.22
6	7	45	50	3	71.6	71.7	−0.13
7	7	45	50	3	70.8	71.7	−0.93
8	9	60	70	2	62.7	62.9	−0.21
9	9	60	30	2	75.9	76.0	−0.14
10	5	60	70	2	72.1	71.6	0.47
11	9	30	70	2	47.8	47.4	0.37
12	3	45	50	3	77.5	78.4	−0.95
13	7	45	50	5	76.0	76.0	−0.02
14	7	45	50	3	71.5	71.7	−0.23
15	5	30	70	2	54.7	54.0	0.66
16	9	60	30	4	83.5	83.8	−0.36
17	9	30	70	4	53.6	54.0	−0.45
18	7	45	10	3	85.0	84.7	0.22
19	7	45	90	3	56.7	57.4	−0.77
20	7	15	50	3	54.4	54.6	−0.20
21	9	60	70	4	69.1	68.4	0.65
22	7	45	50	3	72.0	71.7	0.26
23	7	75	50	3	86.6	86.9	−0.34
24	7	45	50	3	72.0	71.7	0.26
25	5	30	30	2	65.5	65.9	−0.40
26	5	30	30	4	78.6	78.0	0.51
27	11	45	50	3	61.2	60.7	0.40
28	5	30	70	4	64.3	63.9	0.39
29	5	60	30	4	94.8	94.9	−0.12
30	7	45	50	1	57.8	58.3	−0.52

adequacy, and evaluation of significant model terms was done using analysis of variance (ANOVA), Fisher's F test value, and p-value. The coefficient of determination (R^2), adjusted R^2, and predicted R^2 were employed for expressing the goodness of fit of the developed model. Using Equation (5), the number of designed experiments was determined. In the mentioned Equation, k shows the number of variables and Cp is representative of the number of repetitions at the central point (Molla Mahmoudi et al., 2020).

$$N = k^2 + (2 \times k) + C_p \quad (5)$$

Calculation of the percentage effect of each independent variable (P_i) on the degradation of 2,4-DNT was done using Pareto analysis (Eq. (6)) (Samarghandi et al., 2021b):

$$P_i = \left(\frac{\beta_i^2}{\sum \beta_i^2}\right) \times 100 i \neq 0 \quad (6)$$

3. Results and discussion

3.1. Characterization of the G/β-PbO_2 and MCZ@Fe_3O_4 nanoparticles

The morphology of fabricated G/β-PbO_2 electrode with different magnifications was assessed using FESEM (Fig. S1). Based on Fig.(S1), the much smaller grain size, uniform, and compact structure were detected for pyramid crystal-shaped β-PbO_2 particles. Furthermore, the uneven and stratified properties of formed β-PbO_2 on graphite interlayer is led to enhancing the specific surface area of this electrode (Dargahi et al., 2018). EDS elemental analysis was another analysis, which was employed to identify the bulk composition of the synthesized G/β-PbO_2. In Figs (S2, S3), the EDS elemental mapping has been represented based on two major elements present in the surface of the G/β-PbO_2 anode. In elemental mapping, the atomic percentages of lead (Pb) and oxygen (O) were obtained to be 9.91% and 20.09%, respectively. Moreover, based on the EDS spectrum, there is no carbon peak; this reveals the suitably covering of graphite substrate with PbO_2 layers. Through the employment of XRD analysis on anode material prepared, exploration of the phase and crystalline structure of deposited PbO_2 film (Fig. S4) was done. According to the XRD spectrum, the correspondence of all the peaks to β phase and tetragonal symmetry of PbO2 with Joint Committee on Powder Diffraction Standards (JCPDS) card no. 04–005-4491 and 00–041-1492 of the International Centre for Diffraction Data (ICDD) database were proven (Mandal et al., 2018). The diffraction peaks were detected at 2θ = 25.4°, 32°, 36.2°, 40.4°, 45°, 49.2°, 52.2°, 55°, 58.9°, 60°, 62.7°, 67° and 74.5°; these were attributed to (110), (101), (200), (112), (022), (211), (220), (002), (310), (112), (301), (202) and (321) planes of β-PbO_2 (Heidari et al., 2021; Samarghandi et al., 2020).

In Fig. S5 (a), the results related to SEM, which provides the morphological characteristics of MCZ@Fe_3O_4 nanoparticles have been demonstrated; based on this, the non-uniform surface with many pores for MCZ@Fe_3O_4 nanoparticles is detected. Moreover, it is clarified that, after loading of Fe_3O_4 nanoparticles, the surface morphology of the MCZ@Fe_3O_4 nanoparticles has not changed. The XRD pattern (Fig. S5 (b)) at an angle of about 2θ was the device used to estimate the crystalline phase of nanocomposites and characterize their structure, which was indicative of this fact that, in addition to the presence of Montmorillonite (the most and main part of zeolite clinoptilolite), there are non-clay impurities such as Quartz, Calcite, and Feldspar in the structure of the Zeolite. The high crystallinity of the adsorbent was confirmed based on the appearance of sharp and stretched peaks especially at 2θ = 24.5 and 27° (which correspond to clinoptilolite and quartz). The presence of iron oxide particles in the structure of the MCZ@Fe_3O_4 nanoparticle was approved based on the peaks in the X-ray diffraction pattern, which were detected at angles of 30.6°, 35.88°, 43.53°, 53.4°, 57.1°, and 62.6°. The above results finally approve the effective synthesizing of iron oxide particles and coating on zeolite.

3.2. Model development, statistical analysis and optimization of the process

Table 1 represents the statistical combinations of the main variables (i.e., initial pH, particle electrode concentration, current density, and electrolysis time) and the maximum actual and predicted degradation efficiency. Using RSM, experimental results were modeled by second-order polynomial models. Equation (7) represents quadratic models obtained in terms of the coded factors.

$$\begin{aligned} 2,4-DNT degradation(\%) &= +71.73 - 4.42A \\ &+8.08B - 6.83C + 4.42D - 0.5250AB \\ &-0.2250AC - 0.8125AD - 0.0875BC - 0.2750BD \\ &-0.5750CD - 0.5271A^2 - 0.2396B^2 - 0.1521C^2 - 1.14D^2 \end{aligned} \quad (7)$$

By employing the above equation, the response for applied levels of every variable in terms of coded variables can be determined. The high positive value obtained for variables is indicative of a highly positive effect on the response, however, the negative coefficients for the variables indicate an adverse effect on the response. The interaction of factors, which influence the performance of the 3DER process, is determined based on second-order polynomial models. In addition to the quadratic models, validation of empirical models is also done using statistical ANOVA (Bezerra et al., 2008). Through considering five parameters, i.e., the Prob > F of the model, the lack of fit test, adequate precision, adjusted regression coefficient (Adj. R^2), and the regression coefficient (R^2), the validation was done. The significance of the empirical model values is approved by Prob > F; the fitness of the model is assessed based on lack of fit; adequate precision is used to measure the signal-to-noise ratio, and the regression coefficient (R^2) is employed for determining the variability between the actual and predicted results. The values greater than 4 for adequate precision are desirable. Moreover, the selected model is significant and accurate, when the values of R^2 and Adj R^2 values are close. Based on mentioned results in Table 2, the models for degradation of 2,4-DNT could provide results consistent with these criteria. It shows the usability for the prediction of the process performance. In addition, Table 2 clarifies the significance of the CCD model for 2,4-DNT degradation efficiency with an R^2 value of 0.9965. Accordingly, more than 0.96% of the variation of 2,4-DNT degradation efficiency is

Table 2 Statistical models obtained from the analysis of variance for response surface reduced quadratic model for optimization of 2,4-DNT degradation.

Source	Sum of Squares	df	Mean Square	F-value	p-value	
Model	3686.07	14	263.29	584.23	< 0.0001	**significant**
A-pH	468.17	1	468.17	1038.83	< 0.0001	
B-Electrolysis time	1568.17	1	1568.17	3479.66	< 0.0001	
C-2,4-DNT concentration	1117.94	1	1117.94	2480.63	< 0.0001	
D- Current density	469.93	1	469.93	1042.76	< 0.0001	
AB	4.41	1	4.41	9.79	0.0069	
AC	0.8100	1	0.8100	1.80	0.2000	
AD	10.56	1	10.56	23.44	0.0002	
BC	0.1225	1	0.1225	0.2718	0.6097	
BD	1.21	1	1.21	2.68	0.1221	
CD	5.29	1	5.29	11.74	0.0038	
A^2	7.62	1	7.62	16.91	0.0009	
B^2	1.57	1	1.57	3.49	0.0813	
C^2	0.6344	1	0.6344	1.41	0.2539	
D^2	35.62	1	35.62	79.04	< 0.0001	
Residual	6.76	15	0.4507			
Lack of Fit	5.09	10	0.5087	1.52	0.3368	**not significant**
Pure Error	1.67	5	0.3347	**Fit Statistics results:** Std. Dev: 2.67; Mean: 70.09; C.V.%: 5.7; R^2: 0.9982; Adjusted R^2: 0.9965; Predicted R^2: 0.9914; Adeq Precision: 48.83; PRESS: 51.75; **Adequacy of the model tested:** Linear, 2FI, Quadratic and Cubic; **model Suggested: Quadratic**.		
Cor Total	3692.83	29				

explained by the model and the model is not capable of < 0.5% of the variations degradation efficiencies. Following conditions for validation of a model should be observed: Prob > F must be significant (i.e., < 0.05), the lack of fit should be insignificant (i.e., greater than 0.05) and adequate precision should be at least 4. Since the values of P > F were < 0.05, this model was considered to be significant. For 2,4-DNT degradation, A (pH), B (Electrolysis time), C (Current density), and D (2,4-DNT concentration) were significant factors. Moreover, AB (pH × Electrolysis time), AD (pH × 2,4-DNT concentration), CD (Current density × 2,4-DNT concentration), A^2 (pH^2), and D^2 (2,4-DNT concentration^2) were significant model interactions. The regression model variance was evaluated, results of which were described in Fig. 1 (a, b). The distribution of residual points on both sides of the straight line has been clarified, which is indicative of the ordinary distribution of modulus residuals. The error of the used model is typically system error within the permissive error, and the indicated amount of the degradation efficiency from the model can be well-matched with the true degradation efficiency. After analyzing the suitability of the empirical model, prioritization and comparison of the contribution of the operational parameters to the process performance were done using Pareto analysis and Perturbation plots. Specification of the percentage contribution of each factor on 2,4-DNT degradation efficiency as responses was done using Graphical Pareto Analysis according to Eq (6). According to Fig (S6), a significant contribution (28.54 %) for the effect of electrolysis time (B) in 2,4-DNT degradation efficiency was detected. Nonetheless, the lowest contribution (0.31%) in 2,4-DNT degradation efficiency was related to interaction effects electrolysis time × current density (BC). To compare the effect of the operational parameters at a specific point in the design space, perturbation plots were achieved. In these plots, responses are plotted by changing one factor within a selective range while keeping other factors constant. The higher the curvature of the factor is inactive of more sensitivity of the response to that factor. In this study, the plots were at the center of pH (A) = 7, electrolysis time (B) = 45 min, current density (C) = 3 mA/cm^2, and 2,4-DNT concentration (D) = 50 mg/L. According to perturbation plots shown in Fig. 1(c), it was found that 2,4-DNT degradation is the most sensitive to current density (C). Hence, current density has significant effects on response, but electrolysis time (B) has the least.

In this study, the optimization of prediction of 3DER behavior was done using the RSM-CCD method. Four independent input variables were set to "in range" mode and 2,4-DNT degradation efficiency, as the model output was set to "maximum" mode. Among the provided solutions, maximum degradation efficiency for the proposed model was obtained at the first derivative solution. Fig. (S7) shows the optimum conditions obtained (pH = 4.17, electrolysis time = 50.5 min, 2,4-DNT concentration = 23.5 mg/L, current density = 4.8 mA/cm^2) by the RSM-CCD method. By considering these conditions, the highest degradation efficiency of 2,4-DNT by the proposed model was predicted to be 96.05%.

The results related to the reusability of G/β-PbO_2 anode in the studied process used for electrodegradation of 2,4-DNT were presented in Figure (S8).. According to the results presented in Figure (S8), the degradation efficiency in the first oxidation cycle is 98.6%, while it was 94.6% in fifteenth oxidation cycles, which is indicative of only a 4 percent difference between the first and fifteenth cycles; based on this, the good stability and reusability of the prepared anode can be concluded. The higher stability of graphite electrodes can be due to several effective factors as follows: the penetration of lead dioxide particles into the inner layers of the graphite substrate, which causes more interaction and adhesion of the lead dioxide film with the graphite substrate is one of these factors. Another factor, as shown in FESEM (Figures S1) and XRD (Figure S4), is that the reduction in the particle size of β-PbO_2 on the graphite surface can reduce the defect density at the electrode sur-

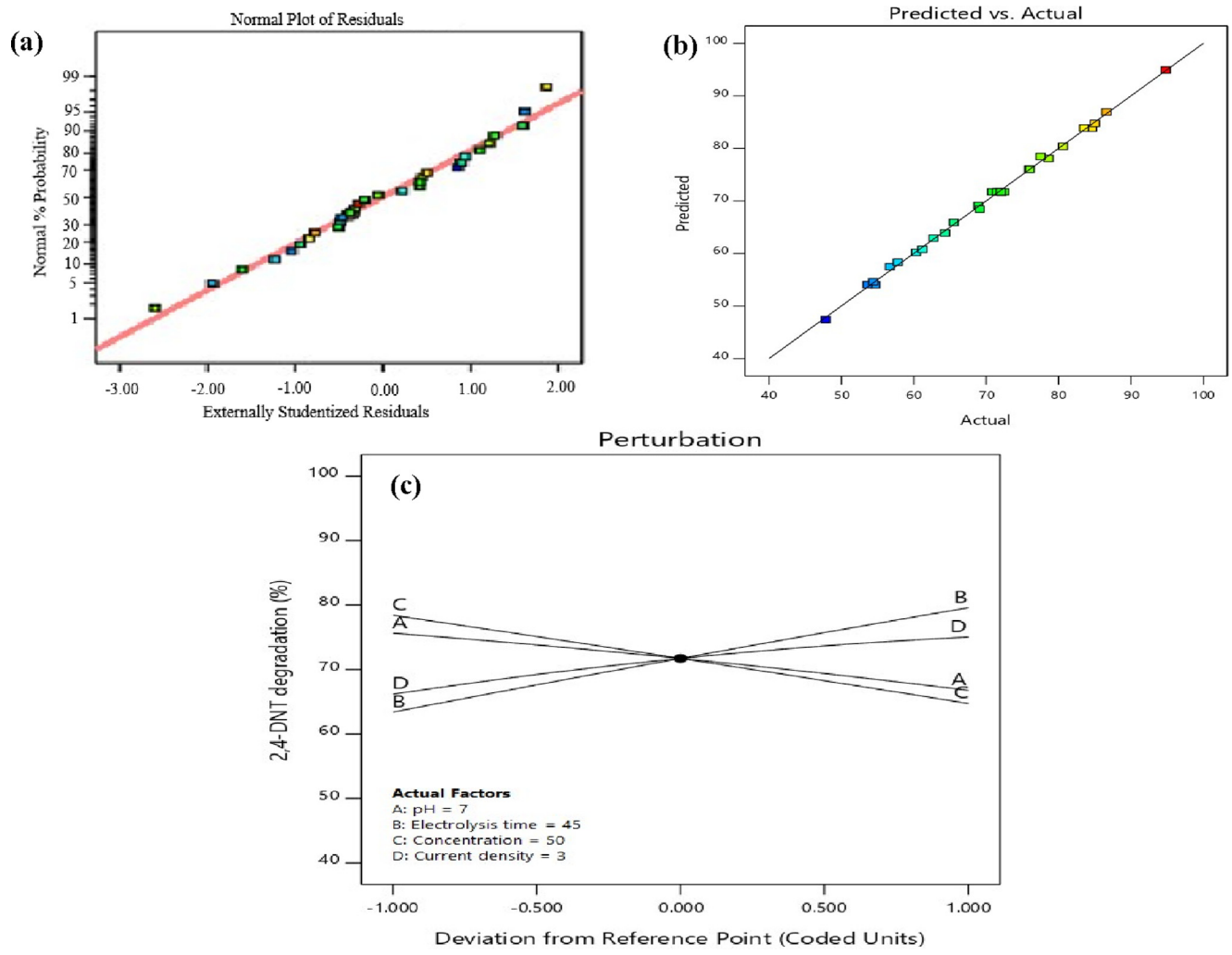

Fig. 1 The diagnostic plots for validation of obtained model: (a) normal plot of residuals, (b) values of 2,4-DNT removal efficiency versus experimental values, and (c) Perturbation plot for 2,4-DNT degradation.

face and create a compact and uniform layer with a micro and dense structure (Dargahi et al., 2019). These results indicate the high electrochemical stability of G/β-PbO_2 electrodes. Therefore, modifying the surface of graphite electrodes and other electrodes prepared with the compact β-PbO_2 film not only eliminates the possibility of electrolyte penetration through cracks and pores but also increases the internal pressure caused by the production of oxygen gas inside the electrode. Therefore, the probability of corrosion, rupture, and mechanical collapse of the electrodes is reduced (Ansari and Nematollahi, 2018; Dargahi et al., 2018).

Moreover, based on results for leaching of lead ion obtained by ICP-MS analysis during the process, the 0.0051 mg/L of lead leaching in the sample solution was detected. This value was much lower than the standards announced by WHO and EPA for drinking water.

In optimum conditions (2,4-DNT concentration = 23.5 mg/L, j = 4.8 mA/cm^2, pH = 4.1, electrolysis time = 50 min, GAC dose = 6 g/250 cc), the value of energy consumption as a function of treated solution volume for 2DER and 3DER-GAC processes was also calculated by Eq. (8) (64, 65). The results showed that the energy consumption for 2DER and 3DER-GAC processes was 5.3 and 2.6 kwh/m^3, respectively. According to the results, the 3DER-GAC has a lower energy consumption compared to 2DER due to high efficiency in the 2,4-DNT degradation, which was even lower than the energy consumption reported in studies conducted by Pipi et al. (2014) (Pipi et al., 2014), Souza et al. (2015) (Souza et al., 2015), Hashim et al. (2017 (Hashim et al., 2017) and Kobya et al. (2016) (Kobya et al., 2016). In the mentioned studies, the energy consumptions were observed to be 16.9, 455.5, 6.21 and 11.17 kwh/m^3, respectively.

$$E_{EC} = \frac{UIt_{EC}}{V_s} \times 10^{-3} \quad (8)$$

Where, E_{EC} is the electrical energy in kWh/m^3, U is the cell voltage in volt (V), I represents the current in ampere (A), t_{EC} is the electrolysis time of the electrochemical process (hr).

3.3. The effect of various parameters

3.3.1. The effect of initial pH

The results of this part of the study, i.e., the effect of pH on the 2,4-DNT removal, were represented in Fig. 2. Based on mentioned Figure, the best DNT removal efficiency (94.85% after

75 min) by the studied system was achieved at a pH of 3, which is agreed with the study conducted by Dargahi et al. (Dargahi et al., 2019). However, an increase in the pH of the samples has led to a remarkable reduction in the removal efficiency. The significant effect of pH on the removal of pollutants has been confirmed by several studies (Ansari and Nematollahi, 2018; Mengelizadeh et al., 2019). This variable can affect the production of various radicals, e.g., hydroxyl radicals (Zhang et al., 2013a). Increasing the production of hydroxyl radical is observed for low values of pH. Enhancing the production of these radicals leads to development in pollutant degradation, which is due to increasing the possibility of contact between these radicals with DNT molecules and higher oxidation power. However, the predominant radicals in very alkaline conditions, especially pH above 12, were the hydroxide radical. The oxidation potential of the hydroxide is harshly declined in alkaline conditions, which is led to diminish the efficiency of the process, even in the presence of the predominant radical. Also, in terms of the degree of radical stability in the aqueous medium, the stability of hydroxide radicals gets much lower (Xie et al., 2021). In the study conducted by Xiu-Yan Li et al., TiO_2-SiO_2/GAC was prepared and used as particle electrodes in a 3DER for the degradation of textile wastewater; in their study (Li et al., 2017), the optimum pH of 3 was also found to be an important parameter for removal of pollutant. Also, in a study conducted by Rahmani et al. for degradation of diuron herbicide in a 3DER with felt/PbO_2 anode, the results showed that with increasing pH, the diuron degradation efficiency decreased (Rahmani et al., 2021), which can be interpreted as follows: As the pH of the solution decreases, the number of produced hydroxyl radicals increases, which have a higher ability for degradation of pollutant in an acidic environment, and therefore the oxidation of organic matter occurs at a higher rate which is consistent with the results of the present study.

3.3.2. The effect of electrolysis time

Increasing electrolysis time in many treatment methods can lead to greater contact between the pollutant and the treatment agent and increase process efficiency. To study the effect of electrolysis time on the degradation of 2,4-DNT, electrolysis time was selected in the range of 15–75 min (Figs. 2 and 3).

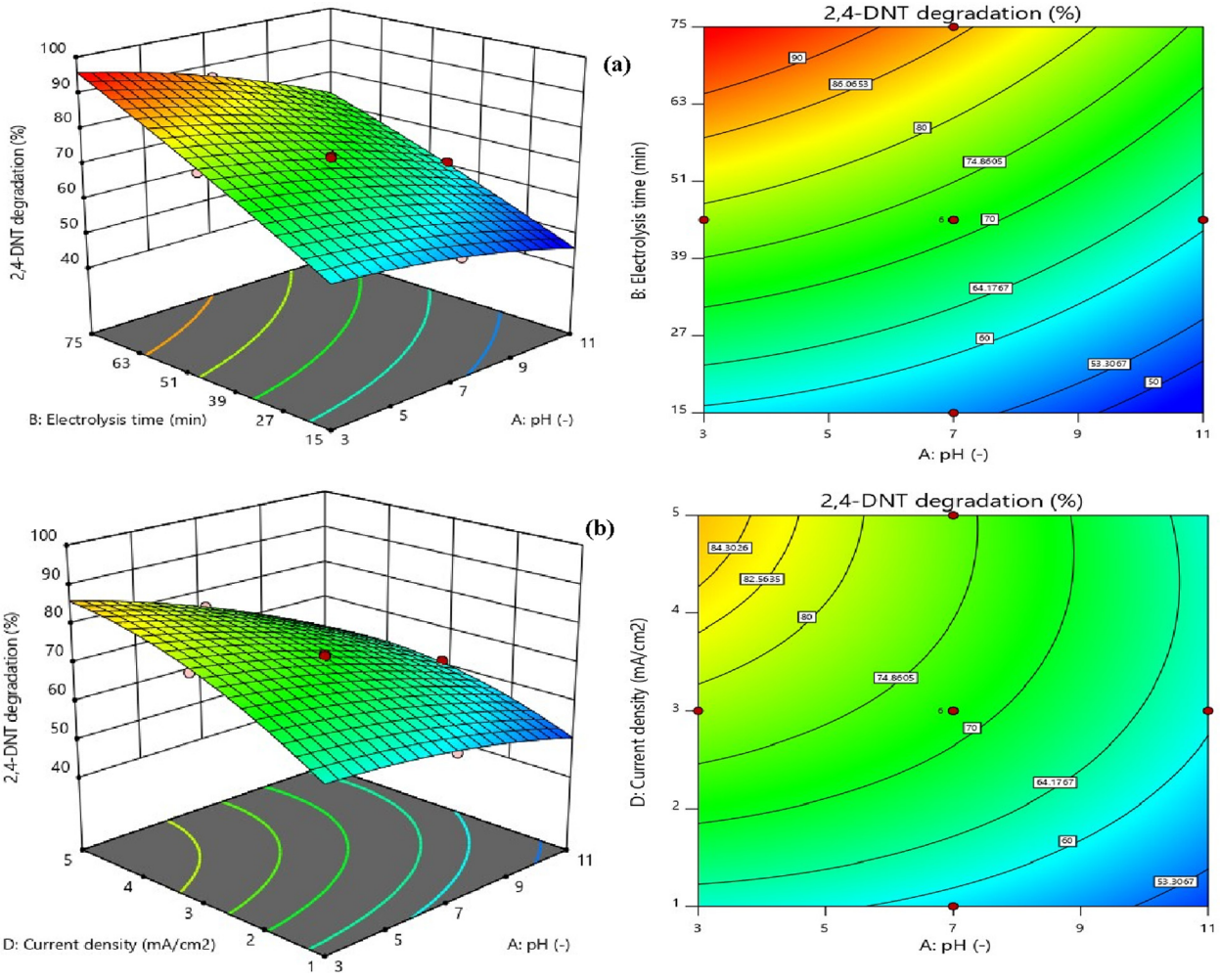

Fig. 2 (a) 3D and contour response surface plots showing the interaction of electrolysis time and pH (2,4-DNT concentration = 50 mg/L, j = 3 mA/cm^2, activated carbon = 6 g/250 cc); (b) 3D and contour response surface plots showing the interaction of Current density and pH (2,4-DNT concentration = 50 mg/L, Electrolysis time = 45 min, Activated carbon = 6 g/250 cc).

According to the results, the electrolysis time was directly correlated with 2,4-DNT degradation efficiency. As the electrolysis time increased, the degradation efficiency of the 2,4-DNT also increased. Because increasing the electrolysis time is led to increasing the amount of hydroxyl radical produced, thereby increasing the efficiency of 2,4-DNT degradation by the electrochemical process (Chabi et al., 2014; Fang et al., 2015; Oudenhoven et al., 2011). Increasing electrolysis time enhances the opportunity to perform Eqs. 9–11, which is led to increasing the contact time of organic pollutants and the intermediates caused by its degradation with $^{\circ}OH$ (Samarghandi et al., 2021b). Improving the performance of 3DER systems in removing organic pollutants by increasing the reaction time has also been reported in studies conducted by Samarghandi et al. (Samarghandi et al., 2021a), Dargahi et al. (Dargahi et al., 2021a; Dargahi et al., 2021d), and Khosravi et al. (Khosravi et al., 2015).

$$O_2 + 2H^+ + 2e^- \rightarrow H_2O_2 \quad (9)$$

$$PbO_2[HO^{\cdot}] + H_2O \rightarrow PbO_2[HO^{\cdot}] + H^+ + e^- \quad (10)$$

$$PbO_2[HO^{\cdot}] + \text{organics} \rightarrow PbO_2[HO^{\cdot}] + mCO_2 + nH_2O + H^+ + e^- \quad (11)$$

3.3.3. The effect of concentration of 2,4-DNT

It is clear that the concentration of pollutants is one of the parameters that varies in different industries. Hence, studying the effect of the initial concentration of pollutants on the degradation efficiency is vital [38–41]. Investigation of the effect of initial 2,4-DNT concentration on 2,4-DNT its degradation efficiency was carried out through conducting the experiments at the initial 2,4-DNT concentrations from 10 to 90 mg/L. The results related to the effect of the initial changes of 2,4-DNT concentration on the efficiency of the 3DER process are presented in Fig. 3. According to the results presented in Fig. 3, there is an inverse relationship between the 2,4-DNT concentration and its degradation efficiency. As the 2,4-DNT concentration decreased from 10 to 90 mg/L, the degradation efficiency of the 2,4-DNT increased from 90.55 to 46.98%. This is consistent with the results of studies by Chen et al.

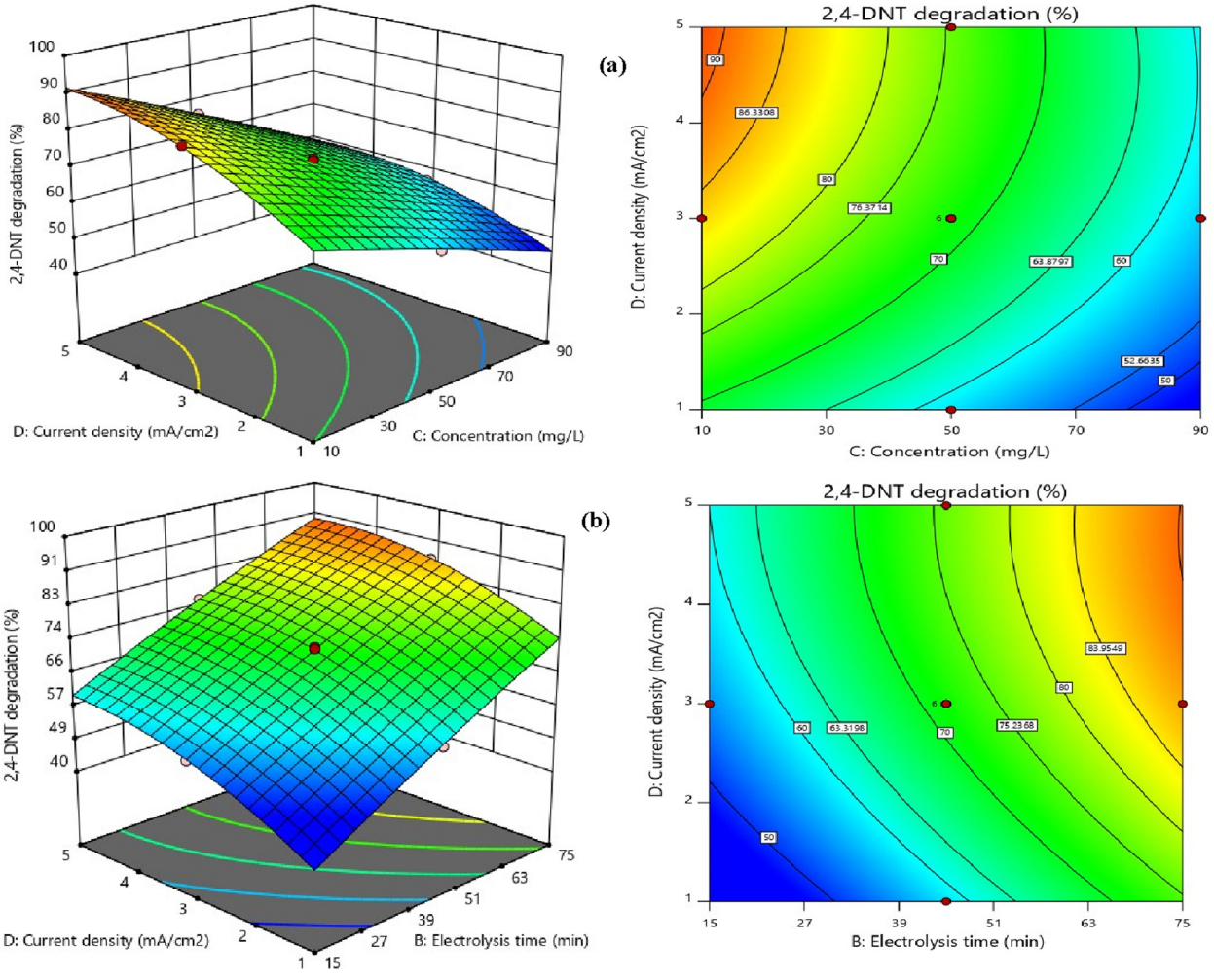

Fig. 3 (a) 3D and contour response surface plots showing the interaction of Current density and 2,4-DNT concentration (pH = 7, electrolysis time = 45 min, activated carbon = 5 g/250 cc), (b) 3D and contour response surface plots showing the interaction of Current density and electrolysis time (2,4-DNT concentration = 50 mg/L, pH = 7, GAC dose = 6 g/250 cc).

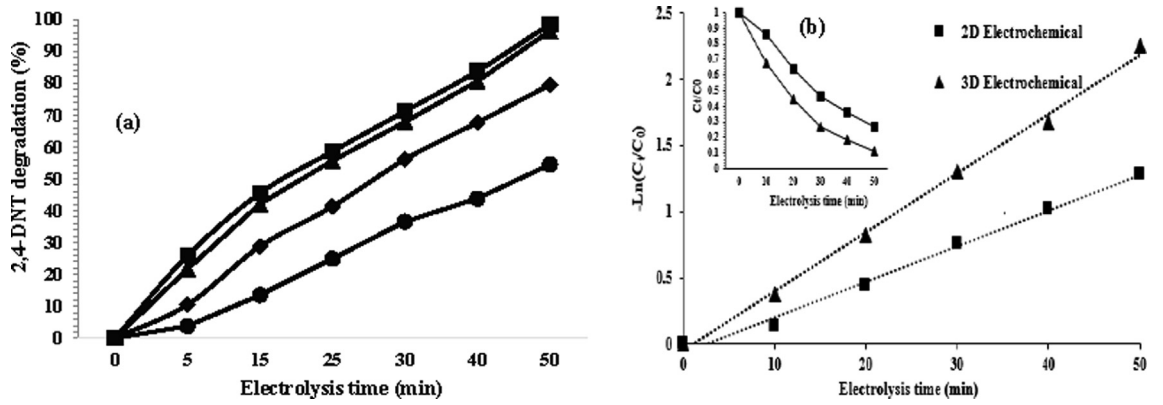

Fig 4 (a) The degradation of 2,4-DNT by the Electrochemical processes (2,4-DNT concentration = 23.5 mg/L, j = 4.8 mA/cm^2, pH = 4.1, GAC and MCZ@Fe_3O_4 nanoparticles dose as particle electrodes = 6 g/250 cc) (■ 3DER with G/β-PbO_2 anode and GAC as particle electrode; ▲3DER with G/β-PbO_2 anode and MCZ@Fe_3O_4 nanoparticles as particle electrode ; ◆ 2DER with G/β-PbO_2 anode; ● 2DER with Graphite anode), (b) Kinetics of 2,4-DNT degradation, (2,4-DNT concentration = 23.5 mg/L, current density = 4.8 mA/cm^2, pH = 4.1, electrolysis time = 50 min, GAC dose = 6 g/250 cc).

(Chen et al., 2011), Samarghandi et al. (Samarghandi et al., 2020), and Jiang et al. (Jiang et al., 2020).

The decrease in the amount of 2,4-DNT degradation by increasing its concentration can be explained as follows: I) since the same conditions have been applied for all samples, the number of hydroxyl radicals produced at each initial concentration of 2,4-DNT was also equal. Therefore, at low concentrations of 2,4-DNT, the hydroxyl radicals can easily remove a large percentage of the contaminants present in the reaction chamber but, by increasing the concentration of the contaminant, the amount of these radicals will be insufficient for its further degradation. 2) The production of intermediates at higher concentrations of 2,4-DNT may also result in competition between the 2,4-DNT molecules and the intermediates with hydroxyl radicals, which leads to reduce removal efficiency [23].**The effect of current density**

The current density (range of 1–5 mA/cm^2) was another evaluated parameter in the present study for the degradation of 2,4-DNT in an aqueous solution. The results showed that there was a direct relationship between current density and 2,4-DNT degradation efficiency. As the current density increased from 1 to 5 mA/cm^2, the degradation efficiency of the 2,4-DNT also increased, and its optimal amount was 4.8 mA/cm^2. At higher current density, more hydroxide radicals are produced for efficient degradation. In this condition, the concentrations of H_2O_2 and $^{\circ}OH$, which are the most important parameters for degradation of DNT, are high and enhance the efficiency of the process. Increasing the current density leads to the production of higher amounts of $HO^{\bullet}$ at the G/β-PbO_2 anode surface, thereby increasing the contaminant removal efficiency. In addition, an increase in current density may lead to an increase in the production rate of $^{\circ}OH$ at the surface of polarized particle electrodes, which also leads to an increase in the indirect oxidation rate of organic pollutants in a 3DER (Guo et al., 2020; Zhang et al., 2013a). Other researchers reported similar results in their studies. For instance, Dargahi et al. observed increased degradation in Moving-bed biofilm reactor combined with three-dimensional electrochemical pretreatment herbicide at the higher current density (Heidari et al., 2021). Also, studies conducted by Ansari et al. (Ansari and Nematollahi, 2018), Bu et al. (Bu et al., 2021), and Pan et al. (Pan et al., 2019) revealed that the pollutant degradation efficiency was increased by increasing current density, which confirms the results of the present study. In spite of the mentioned result, this may be associated with high costs for the treatment of real wastewater (Isaev and Baraboshkin, 1994).

3.4. Synergy of 2,4-DNT degradation and kinetics studies

To clarify the synergy of 2,4-DNT degradation, a comparative study was conducted using 3DER-G/β-PbO_2, 2DER-G/β-PbO_2 anode, 2DER-Graphite anode, and the efficiencies of 2,4-DNT of these systems were compared (Fig. 4a). Based on results obtained under optimal conditions, the 2DER-Graphite anode and 2DER-G/β-PbO_2 anode after 50 min could provide 2,4-DNT degradation efficiencies of 54.5% and 79.5%, respectively. However, under similar operating conditions, the 2,4-DNT degradation efficiency was enhanced to 98.6% and 96.5% in the 3DER-G/β-PbO_2 with GAC and MCZ@Fe_3O_4 nanoparticles as particle electrodes, respectively.

The degradation of 2,4-DNT efficiency using 2DER-G/β-PbO_2 and 2DER-G/β-PbO_2 processes was also estimated based on the rate constants (K), which were studied under optimal conditions (Fig. 4b). Fig. 4b and table (3,) with high R^2 values (R^2 greater than 0.99), was confirmed the applicability of the pseudo-first-order model for explaining the kinetic behavior, which highlighted the remarkable degradation ability of 2DER-G/β-PbO_2 and 2DER-G/β-PbO_2 processes in degradation of 2,4-DNT. Table 3 also represents the half-life ($t_{1/2}$) of 2,4-DNT degradation by evaluated systems. As can

Table 3 The kinetics for the degradation of 2,4-DNT by electrochemical processes at the optimum conditions (2,4-DNT concentration = 23.5 mg/L, j = 4.8 mA/cm^2, pH = 4.1, electrolysis time = 50 min, GAC dose = 6 g/250 cc).

Process	K_{obs} (min^{-1})	R^2	$t_{1/2}$ (min)
2D Electrochemical	0.0217	0.9922	25.95
3D Electrochemical	0.0446	0.9965	15.53

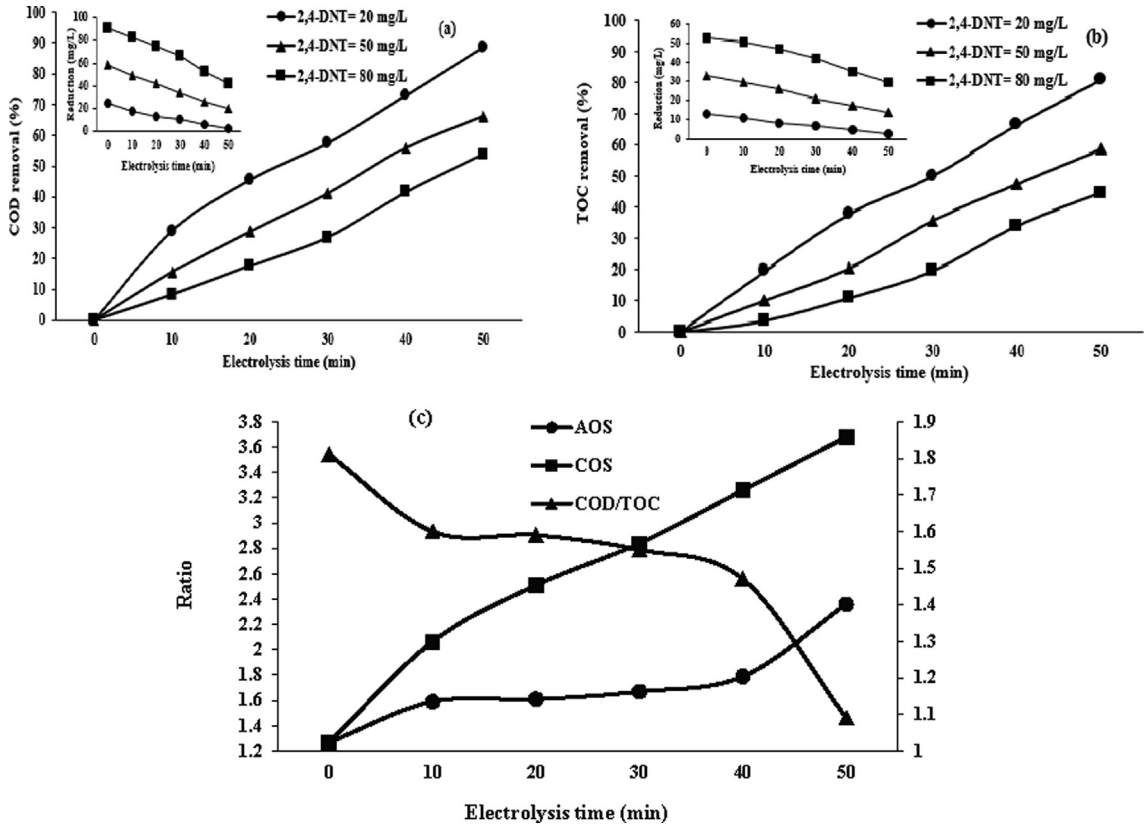

Fig. 5 (a) COD removal, (b) TOC removal (current density = 4.8 mA/cm^2, pH = 4.1, electrolysis time = 50 min, GAC dose = 6 g/250 cc), (c) AOS, COS and COD/TOC of 2,4-DNT in the electrochemical processes process at the optimum conditions (2,4-DNT concentration = 20.0 mg/L, current density = 4.8 mA/cm^2, pH = 4.1, electrolysis time = 50 min, GAC dose = 6 g/250 cc).

be seen its values for the 2DER-G/β-PbO_2 and 2DER-G/β-PbO_2 processes are different and equal to 25.95 and 15.53 min, respectively. Calculation of degradation synergies for the 3DER-G/β-PbO_2 system is performed by placing the kinetic coefficients of 2,4-DNT removal obtained in the 3DER and 2DER oxidation system (represented in Table 3) in the above-mentioned equation (Eq.12) as follow:

$$\text{Synergy}(\%), G/\beta - PbO_2 = \frac{0.0446 - 0.0217}{0.0446} \times 100 = 51.34\% \quad (12)$$

Based on the above, the synergy of evaluated contaminant degradation in 3DER with G/β-PbO_2 anode was 51.34%.

3.5. Mineralization, 2,4-DNT degradation pathway and toxicity testing using bioassay

Evaluation of 2,4-DNT mineralization in the 3DER-GAC system was carried out using G/β-PbO_2 anode based on COD and TOC removal efficiencies at three concentrations of 20, 50, and 80 mg/L 2,4-DNT under optimum conditions, which include the current density of 4.8 mA/cm^2, pH of 4.1, and GAC of 6 g/250 cc (Fig. 5(a, b)). According to the results, increasing electrolysis time has led to significant development of the COD and TOC removal efficiency by the G/β-PbO_2 electrode; so that at the electrolysis time of 10 min, the removal efficiencies of COD and TOC for a 2,4-DNT concentration of 20 mg/L were 28.9% and 19.5%, respectively. However, at the end of 50 min, the removal efficiencies for COD and TOC were 88.5% and 80.9%, respectively. Mentioned results clarified that the electrolysis time had a notable effect on the mineralization of 2,4-DNT. Furthermore, by calculation of parameters, including COD/TOC, AOS, and COS under optimum conditions (2,4-DNT concentration = 20.0 mg/L, current density = 4.8 mA/cm^2, pH = 4.1, electrolysis time = 50 min, and GAC dose = 6 g/250 cc), the biodegradability of 2,4-DNT was assessed. Results related to this part (Fig. 5c) was indicative of an enhancement in the values of AOS (from 1.27 to 2.36) and COS (from 1.27 to 3.68) in the outlet of the 3DER-GAC process and a reduction in the COD/TOC ratio (from 1.81 to 1.09), which confirms the biodegradability of 2,4-DNT by the 3DER-GAC process.

The experiments for determination of the mechanism and intermediates of electrocatalytic oxidation of 2,4-DNT in the studied system were conducted using the pollutant concentration of 25 mg/L in an 0.1 M electrolyte solution (Na_2SO_4) at pH = 5 and a current density of 4.5 mA/cm^2 for 50 min. Through following up the electrolysis process by a Liquid chromatography-mass spectrometry (LC-MS) (Fig. 6), the intermediates were identified and reported in Table 4.

According to the results, masses above 182 are related to the binding of hydroxide to the compound and the production of 2-methyl-3,5-dinitrophenol. Also, by oxidation of the methyl functional group, a combination of 2-hydroxy-4,6-dinitrobenzoic acid with a mass of 228 is produced. In the main process, a methyl group is first isolated and a compound

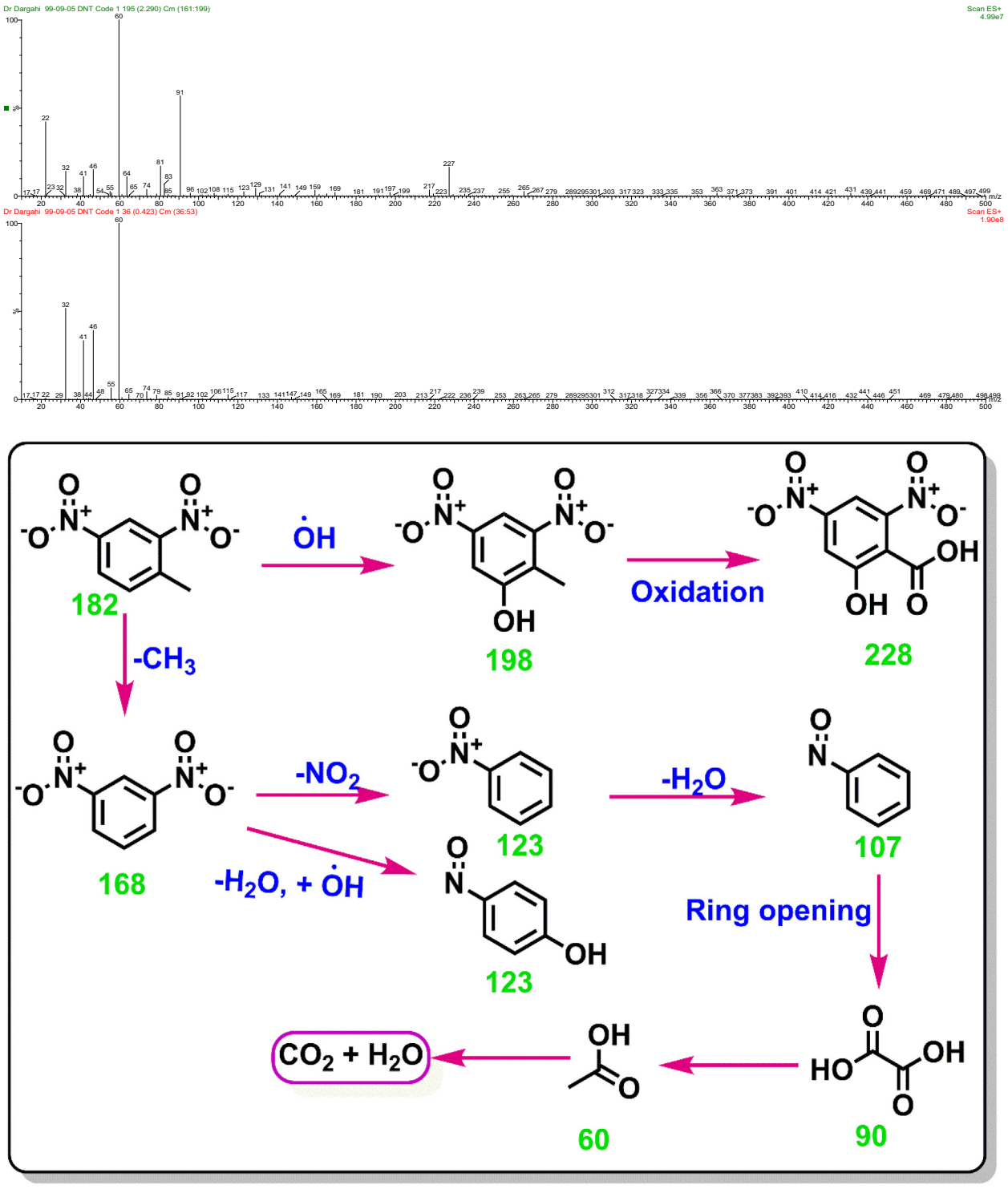

Fig. 6 LC/MS chromatographs and proposed pathway for degradation of 2,4-DNT by 3DER at the optimum condition.

of 1, 3-dinitrobenzene with a mass of 168 is formed. By removal of the nitro group, compounds, i.e., nitrobenzene or 4-nitrosophenol compounds are produced. The opening of the nitrosobenzene compound with a mass of 107 produces oxalic acid and then acetic acid with a mass of 60. The end products of this process are water and carbon dioxide.

To conduct the toxicity tests, the use of standard strains of Gram-negative Escherichia coli (E. coli) and Gram-positive Staphylococcus aureus (S. aureus) were considered (Hasani et al., 2020). Moreover, the broth lactose culture medium was used to perform the toxicity test for degradation of 2,4-DNT by 3DER under the optimal conditions obtained. The

Table 4 Identified intermediates by LC-MS during 2,4-DNT degradation using 3DER with GAC particle electrodes and G/β-PbO_2 anode.

Molecular structure	Chemical name	*m*/*z* (Da)
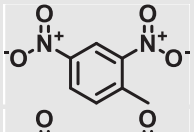	1-methyl-2,4-dinitrobenzene	182
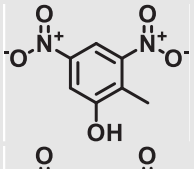	2-methyl-3,5-dinitrophenol	198
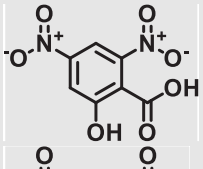	2-hydroxy-4,6-dinitrobenzoic acid	228
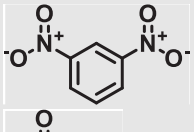	1,3-dinitrobenzene	168
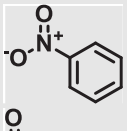	nitrobenzene	123
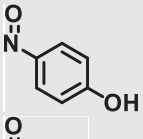	4-nitrosophenol	123
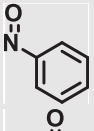	nitrosobenzene	107
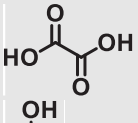	oxalic acid	90
	acetic acid	60

accuracy of the study was confirmed by conducting the experiments in two steps. Lastly, the bacteria growth inhibition in 5 different time intervals were estimated by GI (%) = [(1 – OD_{600S}/OD_{600B}) × 100] for the input and output solutions (Fig. 7). In this equation, GI, OD_{600S}, and OD_{600B} represent the growth inhibition (%), the optical density of the main and control samples at the wavelength of 600 nm, respectively. As reported in Fig. 7, the growth rate of studied bacteria in the control sample and the main effluent was developed after 10 hr, and a decrease in their toxicity was detected. It should be noted that lower bacteria growth was observed in the input solution. Based on the results obtained under optimal conditions including 2,4-DNT concentration = 23.5 mg/L, current density = 4.8 mA/cm^2, pH = 4.1, electrolysis time = 50 min, and GAC dose = 5 g/250 cc, the toxicity rate for E. coli in the reactor inlet solution 55.68% and was decreased to 10.85% for the output solution (80.5% reduction of toxicity) after process. Moreover, the toxicity for S. aureus was 39.82% in the input solution. However, it was reduced to 12.58% in the output solution (68.4% reduction of toxicity) (Table S2).

The results showed that 3DER effectually diminish the toxicity of solution containing 2,4-DNT after treatment, and the bioassay method using microorganisms could be used as an efficient and cost-effective technique to evaluate the toxicity of aqueous solutions. In this study, the reduction of toxicity in gram-positive bacteria was less than gram-negative. In other words, Gram-positive Staphylococcus aureus was less sensitive compared to Escherichia coli in toxicity tests, which may be related to the ability to form spores and cell wall structure in Gram-positive bacteria (Hasani et al., 2020).

4. Conclusions

In this study, a 3DER process was investigated using two different particle electrodes (GAC and MCZ@Fe_3O_4 nanoparticles) to degradation of 2,4-DNT. The results of FESEM, EDS, EDS mapping, and XRD showed that lead oxide was deposited as a film of pyramidal crystals in the form of β-PbO_2 on the graphite surface. RSM-CCD obtained a quadratic model with R^2 greater than 0.99 to predict 2,4-DNT degradation effi-

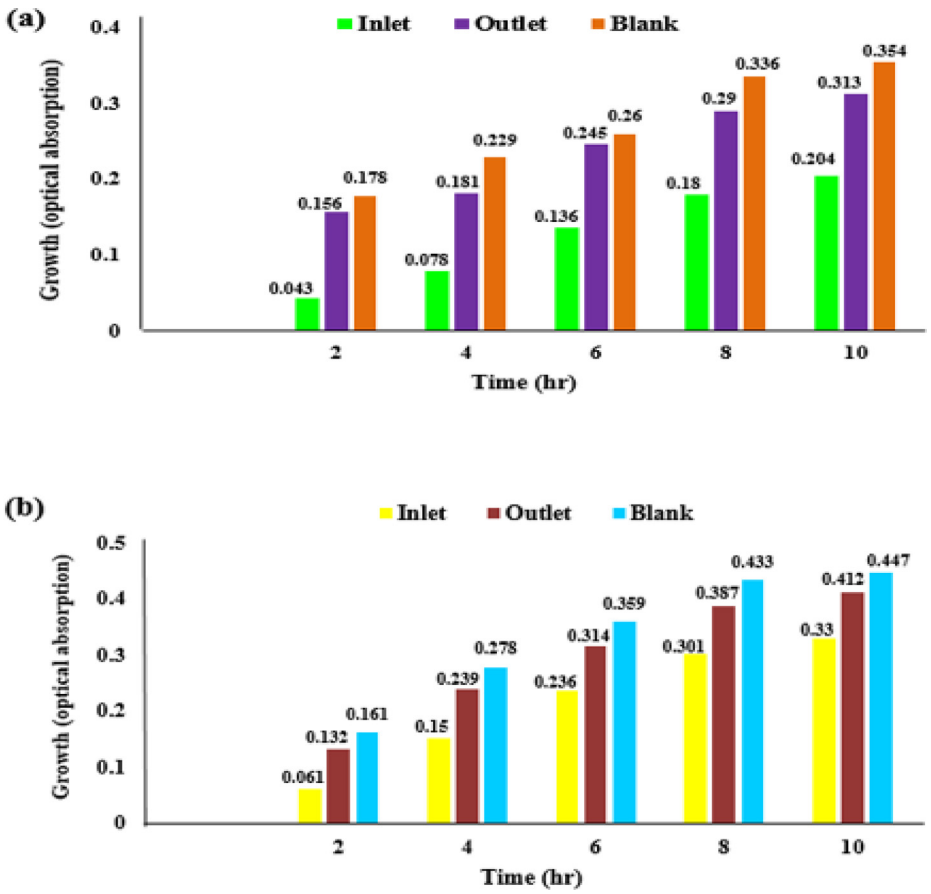

Fig. 7 (a) Growth trend of Escherichia coli (Gram-negative) and (b) Growth trend of Staphylococcus aureus (Gram positive) in toxicity bioassay.

ciency. Accordingly, the optimal conditions for 2,4-DNT concentration, current density, pH, electrolysis time, and GAC dose were 23.5 mg/L, 4.8 mA/cm^2, 4.1, 50 min, and 6 g/250 cc, respectively. Under these conditions, the removal efficiency of 2,4-DNT, COD, and TOC in the 3DER-GAC process were 98.6%, 88.5%, and 80.9%, respectively. The results showed that the parameters of AOS and COS in the effluent of the 3DER-GAC process increased from 1.27 to 2.36 and from 1.27 to 3.68, respectively, which shows the biodegradability of 2,4-DNT by this process. The employment of the mentioned process has a developing trend due to the presence of high concentrations of chemical, synthetic, and toxic pollutants (with an inhibitory effect on the biological activity of microorganisms) and the ability of the system to provide the biodegradability of wastewaters. According to the results, no harmful and toxic byproducts could be detected and the studied pollutant, i.e., 2,4-DNT, was completely degraded to CO_2 and H_2O when the 3DER process with a GAC and MCZ@Fe_3O_4 nanoparticles as particle electrodes and G/β-PbO_2 anode was used for its treatment.

Declaration of Competing Interest

The authors declare that they have no known competing financial interests or personal relationships that could have appeared to influence the work reported in this paper.

Acknowledgments

This work was supported by the Ardabil University of Medical Sciences [grant number IR.ARUMS.REC.1399.243].

Appendix A. Supplementary data

Supplementary data to this article can be found online at https://doi.org/10.1016/j.arabjc.2021.103648.

References

Achtnich, C., Pfortner, P., Weller, M.G., Niessner, R., Lenke, H., Knackmuss, H.-J., 1999. Reductive transformation of bound trinitrophenyl residues and free TNT during a bioremediation process analyzed by immunoassay. Environmental science & technology 33, 3421–3426.

Afshin, S., Rashtbari, Y., Vosough, M., Dargahi, A., Fazlzadeh, M., Behzad, A., Yousefi, M., 2021. Application of Box-Behnken design for optimizing parameters of hexavalent chromium removal from aqueous solutions using Fe3O4 loaded on activated carbon prepared from alga: Kinetics and equilibrium study. Journal of Water Process Engineering 42, 102113.

Ansari, A., Nematollahi, D., 2018. A comprehensive study on the electrocatalytic degradation, electrochemical behavior and degradation mechanism of malachite green using electrodeposited nanostructured β-PbO2 electrodes. Water research 144, 462–473.

Azizi, A., Dargahi, A., Almasi, A., 2021. Biological removal of diazinon in a moving bed biofilm reactor–process optimization with central composite design. Toxin Reviews 40, (4) 1252.

Bezerra, M.A., Santelli, R.E., Oliveira, E.P., Villar, L.S., Escaleira, L. A., 2008. Response surface methodology (RSM) as a tool for optimization in analytical chemistry. Talanta 76, 965–977.

Bradley, P., Chapelle, F., Landmeyer, J., Schumacher, J., 1994. Microbial transformation of nitroaromatics in surface soils and aquifer materials. Applied and Environmental Microbiology 60, 2170–2175.

Bu, J., Deng, Z., Liu, H., Li, T., Yang, Y., Zhong, S., 2021. The degradation of sulfamilamide wastewater by three-dimensional electrocatalytic oxidation system composed of activated carbon bimetallic particle electrode. Journal of Cleaner Production 324, 129256.

Chabi, S., Peng, C., Hu, D., Zhu, Y., 2014. Ideal three-dimensional electrode structures for electrochemical energy storage. Advanced Materials 26, 2440–2445.

Chen, J., Ren, J., Ye, C., Li, L., Yang, C., Qiu, T., 2021. Highly selective removal of 2, 4-dinitrotoluene for industrial wastewater treatment through hyper-cross-linked resins. Journal of Cleaner Production 288, 125128.

Chen, W.-S., Huang, C.-P., 2019. Mineralization of dinitrotoluenes in aqueous solution by sono-activated persulfate enhanced with electrolytes. Ultrasonics sonochemistry 51, 129–137.

Chen, Y., Shi, W., Xue, H., Han, W., Sun, X., Li, J., Wang, L., 2011. Enhanced electrochemical degradation of dinitrotoluene wastewater by Sn–Sb–Ag-modified ceramic particulates. Electrochimica acta 58, 383–388.

Dargahi, A., Ansari, A., Nematollahi, D., Asgari, G., Shokoohi, R., Samarghandi, M.R., 2019. Parameter optimization and degradation mechanism for electrocatalytic degradation of 2, 4-diclorophenoxyacetic acid (2, 4-D) herbicide by lead dioxide electrodes. RSC advances 9, 5064–5075.

Dargahi, A., Hasani, K., Mokhtari, S.A., Vosoughi, M., Moradi, M., Vaziri, Y., 2021a. Highly effective degradation of 2, 4-Dichlorophenoxyacetic acid herbicide in a three-dimensional sono-electro-Fenton (3D/SEF) system using powder activated carbon (PAC)/Fe3O4 as magnetic particle electrode. Journal of environmental chemical engineering 9.

Dargahi, A., Hasani, K., Mokhtari, S.A., Vosoughi, M., Moradi, M., Vaziri, Y., 2021b. Highly effective degradation of 2, 4-Dichlorophenoxyacetic acid herbicide in a three-dimensional sono-electro-Fenton (3D/SEF) system using powder activated carbon (PAC)/Fe3O4 as magnetic particle electrode. Journal of environmental chemical engineering 9, 105889.

Dargahi, A., Nematollahi, D., Asgari, G., Shokoohi, R., Ansari, A., Samarghandi, M.R., 2018. Electrodegradation of 2, 4-dichlorophenoxyacetic acid herbicide from aqueous solution using three-dimensional electrode reactor with G/β-PbO 2 anode: Taguchi optimization and degradation mechanism determination. RSC advances 8, 39256–39268.

Dargahi, A., Samarghandi, M.R., Shabanloo, A., Mahmoudi, M.M., Nasab, H.Z., 2021c. Statistical modeling of phenolic compounds adsorption onto low-cost adsorbent prepared from aloe vera leaves wastes using CCD-RSM optimization: effect of parameters, isotherm, and kinetic studies. Biomass Conversion and Biorefinery, 1–15.

Dargahi, A., Shokoohi, R., Asgari, G., Ansari, A., Nematollahi, D., Samarghandi, M.R., 2021d. Moving-bed biofilm reactor combined with three-dimensional electrochemical pretreatment (MBBR–3DE) for 2, 4-D herbicide treatment: application for real wastewater, improvement of biodegradability. RSC advances 11, 9608–9620.

Epa, 2000. EPA – US Environmental Protection Agency, Priority pollutants. Available from, 08.11.10) http://water.epa.gov/scitech/swguidance/methods/pollutants.cfm(accessed.

Fang, Q., Shen, Y., Chen, B., 2015. Synthesis, decoration and properties of three-dimensional graphene-based macrostructures: a review. Chemical Engineering Journal 264, 753–771.

Geng, R., Chang, R., Zou, Q., Shen, G., Jiao, T., Yan, X., 2021. Biomimetic Nanozymes Based on Coassembly of Amino Acid and Hemin for Catalytic Oxidation and Sensing of Biomolecules. Small 17, 2008114.

Gong, P., Kuperman, R.G., Sunahara, G.I., 2003. Genotoxicity of 2, 4-and 2, 6-dinitrotoluene as measured by the Tradescantia micronucleus (Trad-MCN) bioassay. Mutation Research/Genetic Toxicology and Environmental Mutagenesis 538, 13–18.

Guo, C., Liu, H., Wang, C., Zhao, J., Zhao, W., Lu, N., Qu, J., Yuan, X., Zhang, Y.-N., 2020. Electrochemical removal of levofloxacin using conductive graphene/polyurethane particle electrodes in a three-dimensional reactor. Environmental Pollution 260, 114101.

Hasani, K., Peyghami, A., Moharrami, A., Vosoughi, M., Dargahi, A., 2020. The efficacy of sono-electro-Fenton process for removal of Cefixime antibiotic from aqueous solutions by response surface methodology (RSM) and evaluation of toxicity of effluent by microorganisms. Arabian Journal of Chemistry 13, 6122–6139.

Hashim, K.S., Shaw, A., Al Khaddar, R., Pedrola, M.O., Phipps, D., 2017. Energy efficient electrocoagulation using a new flow column reactor to remove nitrate from drinking water–Experimental, statistical, and economic approach. Journal of environmental management 196, 224–233.

Health, U.D.o., Services, H., 1999. Agency for Toxic Substances and Disease Registry-ATSDR.

Heidari, M., Vosoughi, M., Sadeghi, H., Dargahi, A., Mokhtari, S.A., 2021. Degradation of diazinon from aqueous solutions by electro-Fenton process: effect of operating parameters, intermediate identification, degradation pathway, and optimization using response surface methodology (RSM). Separation Science and Technology 56, 2287–2299.

Hewitt, A.D., Jenkins, T.F., Walsh, M.E., Walsh, M.R., Bigl, S.R., Ramsey, C.A., 2007. Protocols for collection of surface soil samples at military training and testing ranges for the characterization of energetic munitions constituents. ENGINEERING RESEARCH AND DEVELOPMENT CENTER HANOVER NH COLD REGIONS RESEARCH ....

Ibrahim, S., 2017. Experimental Studies on UV Facilitated Photo-Degradation of 2, 4-Dinitrotoluene. California State University, Fullerton.

Isaev, V., Baraboshkin, A., 1994. Three-dimensional electrochemical phase formation. Journal of Electroanalytical Chemistry 377, 33–37.

Jiang, N., Wang, Y., Zhao, Q., Ye, Z., 2020. Application of Ti/IrO2 electrode in the electrochemical oxidation of the TNT red water. Environmental Pollution 259, 113801.

Jiang, N., Zhao, Q., Xue, Y., Xu, W., Ye, Z., 2018. Removal of dinitrotoluene sulfonate from explosive wastewater by electrochemical method using Ti/IrO2 as electrode. Journal of Cleaner Production 188, 732–740.

Khosravi, R., Fazlzadehdavil, M., Barikbin, B., Hossini, H., 2015. Electro-decolorization of Reactive Red 198 from aqueous solutions using aluminum electrodes systems: modeling and optimization of operating parameters. Desalination and Water Treatment 54, 3160.

Kobya, M., Gengec, E., Demirbas, E., 2016. Operating parameters and costs assessments of a real dyehouse wastewater effluent treated by a continuous electrocoagulation process. Chemical Engineering and Processing: Process Intensification 101, 87–100.

Kuşçu, Ö.S., Sponza, D.T., 2011. Application of Box-Wilson experimental design method for 2, 4-dinitrotoluene treatment in a sequential anaerobic migrating blanket reactor (AMBR)/aerobic completely stirred tank reactor (CSTR) system. Journal of hazardous materials 187, 222–234.

Li, J., Yan, J., Yao, G., Zhang, Y., Li, X., Lai, B., 2019. Improving the degradation of atrazine in the three-dimensional (3D) electrochem-

ical process using CuFe2O4 as both particle electrode and catalyst for persulfate activation. Chemical Engineering Journal 361, 1317–1332.

Li, X.-Y., Xu, J., Cheng, J.-P., Feng, L., Shi, Y.-F., Ji, J., 2017. TiO2-SiO2/GAC particles for enhanced electrocatalytic removal of acid orange 7 (AO7) dyeing wastewater in a three-dimensional electrochemical reactor. Separation and Purification Technology 187, 303–310.

Liu, C., Lin, Y., Dong, Y., Wu, Y., Bao, Y., Yan, H., Ma, J., 2020. Fabrication and investigation on Ag nanowires/TiO 2 nanosheets/-graphene hybrid nanocomposite and its water treatment performance. Advanced Composites Hybrid Materials 3, 402–414.

Ma, Z., Yang, Y., Jiang, Y., Xi, B., Yang, T., Peng, X., Lian, X., Yan, K., Liu, H., 2017. Enhanced degradation of 2, 4-dinitrotoluene in groundwater by persulfate activated using iron–carbon micro-electrolysis. Chemical Engineering Journal 311, 183–190.

Mandal, P., Gupta, A.K., Dubey, B.K., 2018. A novel approach towards multivariate optimization of graphite/PbO2 anode synthesis conditions: Insight into its enhanced oxidation ability and physicochemical characteristics. Journal of environmental chemical engineering 6, 4438–4451.

Mao, R., Zhao, X., Lan, H., Liu, H., Qu, J., 2015. Graphene-modified Pd/C cathode and Pd/GAC particles for enhanced electrocatalytic removal of bromate in a continuous three-dimensional electrochemical reactor. Water research 77, 1–12.

Mengelizadeh, N., Pourzamani, H., Saloot, M.K., Hajizadeh, Y., Parseh, I., Parastar, S., Niknam, N., 2019. Electrochemical degradation of reactive black 5 using three-dimensional electrochemical system based on multiwalled carbon nanotubes. Journal of Environmental Engineering 145, 04019021.

Molla Mahmoudi, M., Khaghani, R., Dargahi, A., Monazami Tehrani, G., 2020. Electrochemical degradation of diazinon from aqueous media using graphite anode: Effect of parameters, mineralisation, reaction kinetic, degradation pathway and optimisation using central composite design. International Journal of Environmental Analytical Chemistry, 1–26.

Oh, S.-Y., Kang, S.-G., Chiu, P.C., 2010. Degradation of 2, 4-dinitrotoluene by persulfate activated with zero-valent iron. Science of The Total Environment 408, 3464–3468.

Oudenhoven, J.F., Baggetto, L., Notten, P.H., 2011. All-solid-state lithium-ion microbatteries: a review of various three-dimensional concepts. Advanced Energy Materials 1, 10–33.

Pan, G., Jing, X., Ding, X., Shen, Y., Xu, S., Miao, W., 2019. Synergistic effects of photocatalytic and electrocatalytic oxidation based on a three-dimensional electrode reactor toward degradation of dyes in wastewater. Journal of Alloys Compounds 809, 151749.

Patapas, J., Al-Ansari, M.M., Taylor, K., Bewtra, J., Biswas, N., 2007. Removal of dinitrotoluenes from water via reduction with iron and peroxidase-catalyzed oxidative polymerization: a comparison between Arthromyces ramosus peroxidase and soybean peroxidase. Chemosphere 67, 1485–1491.

Pedersen, N.L., Fini, M.N., Molnar, P.K., Muff, J., 2019. Synergy of combined adsorption and electrochemical degradation of aqueous organics by granular activated carbon particulate electrodes. Separation and Purification Technology 208, 51–58.

Pipi, A.R., Sirés, I., De Andrade, A.R., Brillas, E., 2014. Application of electrochemical advanced oxidation processes to the mineralization of the herbicide diuron. Chemosphere 109, 49–55.

Rahmani, A., Leili, M., Seid-Mohammadi, A., Shabanloo, A., Ansari, A., Nematollahi, D., Alizadeh, S., 2021. Improved degradation of diuron herbicide and pesticide wastewater treatment in a three-dimensional electrochemical reactor equipped with PbO2 anodes and granular activated carbon particle electrodes. Journal of Cleaner Production 322, 129094.

Reddy, G.K.K., Sarvajith, M., Nancharaiah, Y., Venugopalan, V., 2017. 2, 4-Dinitrotoluene removal in aerobic granular biomass sequencing batch reactors. International Biodeterioration & Biodegradation 119, 56–65.

Report, 2010. Technical report: Data on the European Market, Uses and Releases/Exposures for 2,4-Dinitrotoluene prepared for ECHA by DHI in co-operation with Risk & Policy Analysts Limited and TNO (Contract ECHA/2008/2/SR25), 11 June 2010.

Rocheleau, S., Kuperman, R.G., Simini, M., Hawari, J., Checkai, R. T., Thiboutot, S., Ampleman, G., Sunahara, G.I., 2010. Toxicity of 2, 4-dinitrotoluene to terrestrial plants in natural soils. Science of The Total Environment 408, 3193–3199.

Samarghandi, M.R., Ansari, A., Dargahi, A., Shabanloo, A., Nematollahi, D., Khazaei, M., Nasab, H.Z., Vaziri, Y., 2021a. Enhanced electrocatalytic degradation of bisphenol A by graphite/β-PbO2 anode in a three-dimensional electrochemical reactor. Journal of environmental chemical engineering 9, 106072.

Samarghandi, M.R., Dargahi, A., Rahmani, A., Shabanloo, A., Ansari, A., Nematollahi, D., 2021b. Application of a fluidized three-dimensional electrochemical reactor with Ti/SnO2–Sb/β-PbO2 anode and granular activated carbon particles for degradation and mineralization of 2, 4-dichlorophenol: Process optimization and degradation pathway. Chemosphere 279, 130640.

Samarghandi, M.R., Dargahi, A., Shabanloo, A., Nasab, H.Z., Vaziri, Y., Ansari, A., 2020. Electrochemical degradation of methylene blue dye using a graphite doped PbO2 anode: optimization of operational parameters, degradation pathway and improving the biodegradability of textile wastewater. Arabian Journal of Chemistry 13, 6847–6864.

Seidmohammadi, A., Vaziri, Y., Dargahi, A., Nasab, H.Z., 2021. Improved degradation of metronidazole in a heterogeneous photo-Fenton oxidation system with PAC/Fe3O4 magnetic catalyst: biodegradability, catalyst specifications, process optimization, and degradation pathway. Biomass Conversion and Biorefinery, 1–17.

Shukla, N., Gupta, V., Rawat, A.S., Gahlot, V.K., Shrivastava, S., Rai, P.K., 2018. 2, 4-Dinitrotoluene (DNT) and 2, 4, 6-Trinitrotoluene (TNT) removal kinetics and degradation mechanism using zero valent iron-silica nanocomposite. Journal of environmental chemical engineering 6, 5196–5203.

Souza, F., Saéz, C., Lanza, M.R., Cañizares, P., Rodrigo, M., 2015. Removal of herbicide 2, 4-D using conductive-diamond sono-electrochemical oxidation. Separation and Purification Technology 149, 24–30.

Sugashini, S., Begum, K.M.S., 2013. Optimization using central composite design (CCD) for the biosorption of Cr (VI) ions by cross linked chitosan carbonized rice husk (CCACR). Clean Technologies and Environmental Policy 15, 293–302.

Tchounwou, P.B., Wilson, B.A., Ishaque, A.B., Schneider, J., 2001. Transcriptional activation of stress genes and cytotoxicity in human liver carcinoma cells (HepG2) exposed to 2, 4, 6-trinitrotoluene, 2, 4-dinitrotoluene, and 2, 6-dinitrotoluene. Environmental Toxicology: An International Journal 16, 209–216.

Tian, F., Geng, S., He, L., Huang, Y., Fauzi, A., Yang, W., Liu, Y., Yu, Y., 2021. Interface engineering: PSS-PPy wrapping amorphous Ni-Co-P for enhancing neutral-pH hydrogen evolution reaction performance. Chemical Engineering Journal 417, 129232.

Venkatadri, R., Peters, R.W., 1993. Chemical oxidation technologies: ultraviolet light/hydrogen peroxide, Fenton's reagent, and titanium dioxide-assisted photocatalysis. Hazardous waste and hazardous materials 10, 107–149.

Wang, C., Xu, C., Sun, W., Liu, F., Yu, S., Xian, M., 2017. Effective adsorption of nitroaromatics at the low concentration by a newly synthesized hypercrosslinked resin. Water Science and Technology 76, 2328–2336.

Wang, Y., Xie, W., Liu, H., Gu, H., 2020. Hyperelastic magnetic reduced graphene oxide three-dimensional framework with superb oil and organic solvent adsorption capability. Advanced Composites Hybrid Materials 3, 473–484.

Xiao, H., Liu, R., Zhao, X., Qu, J., 2008. Enhanced degradation of 2, 4-dinitrotoluene by ozonation in the presence of manganese (II) and oxalic acid. Journal of Molecular Catalysis A: Chemical 286, 149–155.

Xie, W., Shi, Y., Wang, Y., Zheng, Y., Liu, H., Hu, Q., Wei, S., Gu, H., Guo, Z., 2021. Electrospun iron/cobalt alloy nanoparticles on carbon nanofibers towards exhaustive electrocatalytic degradation of tetracycline in wastewater. Chemical Engineering Journal 405, 126585.

Xu, X., Xi, B., Zhang, Y., Xia, F., Han, X., Gao, P., Wan, S., Jiang, Y., Yang, Y., 2020. A comparative study on the treatment of 2, 4-dinitrotoluene contaminated groundwater in the combined system: efficiencies, intermediates and mechanisms. Science of The Total Environment 735, 139161.

Xu, X., Yang, Y., Jia, Y., Lian, X., Zhang, Y., Feng, F., Liu, Q., Xi, B., Jiang, Y., 2019. Heterogeneous catalytic degradation of 2, 4-dinitrotoluene by the combined persulfate and hydrogen peroxide activated by the as-synthesized Fe-Mn binary oxides. Chemical Engineering Journal 374, 776–786.

Yin, J., Ge, B., Jiao, T., Qin, Z., Yu, M., Zhang, L., Zhang, Q., Peng, Q., 2021. Self-assembled sandwich-like MXene-derived composites as highly efficient and sustainable catalysts for wastewater treatment. Langmuir 37, 1267–1278.

Yuanbi, Z., Zumin, Q., Huang, J., 2008. Preparation and analysis of Fe3O4 magnetic nanoparticles used as targeted-drug carriers. Chinese Journal of Chemical Engineering 16, 451–455.

Zhang, C., Jiang, Y., Li, Y., Hu, Z., Zhou, L., Zhou, M., 2013a. Three-dimensional electrochemical process for wastewater treatment: a general review. Chemical Engineering Journal 228, 455–467.

Zhang, C., Xie, Y., Deng, H., Zhang, C., Su, J.-W., Lin, J., 2019. Nitrogen doped coal with high electrocatalytic activity for oxygen reduction reaction. Engineered Science 8, 39–45.

Zhang, J., Wang, S.-Y., Ma, Y.-Y., Chen, L.-P., Chen, W.-H., 2020. Investigation of the decomposition kinetics and thermal hazards of 2, 4-Dinitrotoluene on simulation approach. Thermochimica Acta 684, 178350.

Zhang, Y., Wang, X., Lv, F., Chu, P.K., Ye, Z., Zhou, F., Zhang, R., Wei, F., 2013b. Adsorption behavior and mechanism of 2, 4, 6-trinitrotoluene by functionalized polystyrene nanospheres. Journal of applied polymer science 128, 3720–3725.

Zhao, Q., Ye, Z., Zhang, M., 2010. Treatment of 2, 4, 6-trinitrotoluene (TNT) red water by vacuum distillation. Chemosphere 80, 947–950.